A novel solar concentrator system for combined heat and power application in residential sector

This paper was presented at the 7th International Conference on Applied Energy (ICAE2015), March 28-31, 2015, Abu Dhabi, UAE (Original paper title: "**Energetic and Economic Analysis of a New Concept of Solar Concentrator for Residential Application**" and Paper No.: **ICAE2015-342**

A NOVEL SOLAR CONCENTRATOR SYSTEM FOR COMBINED HEAT AND POWER APPLICATION IN RESIDENTIAL SECTOR

M. Bianchi[a], E. Diolaiti[b], A. Giannuzzi[b], B. Marano[c], F. Melino[a,*], A. Peretto[a]

[a] DIN – Alma Mater Studiorum, viale del Risorgimento 2, 40136, Bologna

[b] INAF – Osservatorio Astronomico di Bologna, via Ranzani 1, 40127, Bologna

[c] DIFA – Alma Mater Studiorum, viale Berti Pichat 6/2, 40127, Bologna

*corresponding author: e-mail: francesco.melino@unibo.it, phone: +39-051-2093318

ABSTRACT

The research on photovoltaic conversion is continuously overtaking technological challenges and modern PV cells can nowadays be efficiently combined with solar concentrators. In this paper a new photovoltaic solar concentrator model based on non-imaging optics and embedding high efficiency multi-junctions cells is presented. The concentrator has been optimized to maximize the electricity production but it is thought to work in cogeneration to allow also for thermal energy by recovering the residual heat, since an active cooling system for the cells is necessary. The maximization is performed by applying deformations to standard spherical mirrors in order to manage solar aberrations and reshape the solar spot . The induced deformations solve issues related to the disuniformity of the spot focused at the receiver consisting of a dense array of cells thus boosting the conversion efficiency. The efficiency enhancing is obtained thanks to the high matching between the collected solar irradiance and the receiver electrical features. An analytical study, considering residential utilities has been performed in order to understand the energetic and economic performance of the system. In particular, a simulation has been carried out by the use of an in-house-developed calculation code considering a whole year of operation in order to estimate the electrical and thermal energy which can be produced by the solar concentrator and self-consumed by the utilities. Further, the maximum capital cost of the system has been estimated in order to achieve a return of the investment in ten or twelve years.

Keywords: Renewable Energy; Solar Concentration; Non Imaging Optics; Combined Heat and Power; Feasibility Study

NOMENCLATURE

Abbreviation

AB	Auxiliary Boiler
CC	Compression Chiller
CPV	Concentrating Photovoltaic
CHP	Combined Heat and Power
ES	Electrical Storage
ICE	Internal Combustion Engine
MGT	Micro Gas Turbine
MJ	Multi-Junction
MRC	Micro Rankine Cycle
SC	SOLARIS Concentrator
SE	Stirling Engine
SO	Secondary Optic

Symbols

C	Capital Cost [€]
DNI	Direct Normal Irradiance [kW/m^2]
E	Energy [kWh]
F	Cash Flow [€]
FFS	Fossil Fuel Saving [kWh]
i	Discount Rate [-]
M	Mass [Sm^3]
n	Year
NPV	Net Present Value [€]
η	Efficiency [-]
ζ	Specific Cost [€/kWh or €/Sm^3]

Subscripts and Superscripts

EL	Electrical
g	Natural Gas (fuel)
R	Reference
TH	Thermal
u	Utility

1. INTRODUCTION

The renewable electricity production increased rapidly during the last decades, but the yearly installed capacity of Concentrating Photovoltaic (CPV) systems [1] had a significant increasing only during the last few years [2]. The crucial driver of this trend is the development of multi-junction (MJ) solar cells with efficiency higher and higher. Despite MJ cells are mainly addressed to powering satellites, cost effectiveness for terrestrial use has been demonstrated when they are employed together with solar concentration [3] especially in very insulated environments or off-grid communities. Currently, a record efficiency above 45% has been obtained for terrestrial type cells [4]. Among the concentrating systems commercially available embedding MJ cells, the dense array systems consist in a large reflective element (called dish) focusing the light over an module of cells arranged one beside the other and electrically connected (mainly in series) to form a single PV receiver. As in the more diffused single cell point focus systems represented by the Fresnel lens based devices [5-7], the whole mechanical structure has to accurately track the sun during its daily motion and to make the light rays exactly converging onto the focal plane. To reproduce defined concentration level and spot shape, a mosaic of low cost flat mirrors mounted on a unique frame is often employed. Mirrored dishes with diameters ranging from few to tens of meters have been developed and commercialized during the last ten years working at typical concentration of 500 suns [8-10] even if recent studies shown a good prospective of increasing the concentration factor towards 1000 suns and beyond [11]. Advantages of the reflective optics are the lack of chromatic aberration, which gives an higher optical efficiency if compared to systems embedding lenses, a lower cell operating temperature caused by the necessary active cooling and the possibility to cogenerate both heat and current given by the cooling system itself. Another advantage, when compared to other CPV technologies, is in the possibility to remove the receiver in case of cleaning, testing or in case of maintenance and, as solar cell technology improves, to upgrade the whole PV system by replacing the receiver with an higher efficiency device at very low cost.

As the conversion efficiency is the main driver of the CPV technology economic sustainability, an important issue in projecting dense array systems is represented by the irradiance distribution over the array, a problem widely discussed in bibliography for single cell systems [12] but less investigated for dense arrays [13, 14]. A non-uniform irradiance pattern could severely worsen the receiver electrical performance thereby reducing the efficiency. The current produced by the worst illuminated cell limits the series output current. The cell can be also subject to an overheating due to the dissipation of extra current from other cells and can eventually break out. The irradiance pattern should rather be as uniform as possible and, at the same time, the spot shape should resemble the typical rectangular/square shape of the array to prevent spillage losses. Flux uniformity and spot reshaping are theoretically possible by redesigning the optics of a concentrator using non-imaging optics [15], by approximating standard imaging mirrors with an array of flat elements, as commonly done in the dishes [16], and/or by adding secondary optics (SOs) to tailor the flux delivered by the dish [17, 18]. At present, no commercial systems seems to embed SOs coupled with dense arrays.

A CPV dense array concentrator model based on a new optical concept has been briefly described in this work [19]. The design method used has been conceived to reduce the current mismatch problem by acting on the optical part. The simulation results shows both high irradiance uniformity and high concentration at the focal plane so that the nominal conversion efficiency of the receiver almost equals the performance of the embedded cells. The proposed system has been evaluated with a series of simulations in order to understand its potential as renewable micro-CHP generator with reference to residential utilities. The electrical and thermal energy production and the maximum sustainable capital cost of the system have been calculated and will be discussed in the next sections of this paper.

2. THE SOLARIS CONCENTRATOR MODELING

The SOLARIS concentrator [19] has been conceived as a single stage multi-dish reflective optics made by mirrors: seven mirrors substitute the traditional segmented dish, focusing the light at the same point so that the final illumination pattern impinging on the receiver results from the sum of the single incoherent illumination produced. Each mirror is a free-form optics, a type of optics often used for solving the prescribed irradiance problem in lenses of limited dimensions often used as SOs. The design guideline is to introduce controlled deformations into originally spherical mirrors in order to degrade the solar image thus obtaining a square spot with prescribed and highly uniform irradiance distribution. Since an accurate imaging formation is not necessary for a concentrator to work, the radiation bundle redistribution aims at maximizing the conversion efficiency by matching the spot with receiver features.

The system optical/electrical modelling has been carried out with an end-to-end code written on purpose in Interactive Data Language IDL® based on analytical models for both the optics and the receiver including two main subgroups of routines for individually simulating each part. A third group of procedures calculates the tolerances for the optical/mechanical parameters. As for the optics, all mirrors have been simulated and designed implementing in the code a well-known analytical model of aberrations based on the Zernike polynomials [20]. Considering a single spherical mirror, a preliminary optical analysis showed that very few deformations associated by coefficients to the Zernike modes, can boost the irradiance uniformity starting from the intrinsically circular solar image (Figure 1). For a single spherical mirror focusing on axis we identified three polynomials: the 4th, the 11th and the 14th, corresponding precise deformations to be applied to a mirror working defocused as shown in Table 1. Then, we extended the method to a multi-mirror system, including off-axis mirrors distributed on an hexagonal frame and other polynomials. Ray tracing techniques have been implemented to simulate and optimize simultaneously all the reflective surfaces. Each step of the optical modeling and the results have been further checked with the optical design software Zemax® as reference.

The receiver has been analytically designed and numerically simulated using a datasheet of commercially available MJ cells 3C40 produced by AZUR SPACE [21] with 39% nominal efficiency at 500 suns at ambient temperature. The electrical scheme employs series/parallels standard electrical connections. Since the cells include busbars, part of the concentrated light will necessary impinge on the these inactive areas: the nominal efficiency considering the cell embedded in a dense array is thus reduced to around 33%. This new value has to be also accounted as the maximum efficiency theoretically obtainable by an array made with this specific cells.

The concentrator has been dimensioned as a power system suitable for the market of medium residential contexts or small farms, then for a production of around 10 kW_{EL}. The diameter of the single mirror has been set 2.6 m, for a system total size of about 7.8 m and a resulting total optical area slightly bigger than 35 m^2. Supposing a standard test direct irradiance of 1 kW/m^2 (1 sun), the collected power will be around 35 kW: with an ideal receiver working at the efficiency of the considered cells, such a system would deliver more than 10 kWe. The detector distance has been set to 4.8 m in order to have a detector distance to total diameter ratio (parameter similar to the focal ratio in imaging systems) of 0.6. In general, small focal ratios are preferred by concentrator designes despite of the higher aberrations introduced in order to achieve high concentration and mechanical structure compactness.

3. EFFICIENCY OPTIMIZATION AND PERFORMANCE ANALYSIS

The concentrator has been optimized for an average concentration of 500 suns where the cell efficiency curve has a maximum. Figure 2 depicts the mechanical model of the system and a zoom of the focal zone, where the receiver electrical scheme has been superimposed to the irradiance pattern simulated after the optimization. The narrow rectangles in figure are strings of cells series connected. Groups of strings are then parallel connected(not shown in figure) to ensure small parallel mismatches and to obtain high voltage and small current in output. This condition is always imposed to avoid excessive current dissipation. The electric model used has ideally no dependence from temperature and spectral variation. Since we deal exclusively with reflective elements no chromatic aberration is introduced, so the last assumption is realistic. The temperature can also be considered reasonably constant as efficient cooling systems have been already investigated, as shown in literature [22, 23].

The performance curves of the system are presented from Figure 3 to Figure 6. In particular, Figure 3 shows both the power collected by the concentrator (input power) and the light effectively impinging on the array (collected power). It should be observed that, at this stage, no model for the bypass diode has been implemented. The mirrors shapes optimized to maximize the efficiency of this receiver gives a uniform irradiance pattern over the 80% of the total power focused (red zone in Figure 2).

The net produced electrical and thermal powers are presented in Figure 4. It can be observed from the figure that the trend of the curves is linear with the variation of the direct normal irradiance, varying from zero to about 10.4 kW_{EL} and 22.8 kW_{TH} respectively for what regards the electrical and thermal power output of the SOLARIS concentrator.

Due to the high matching between light and cells, the receiver shows an effective electrical conversion efficiency (see Figure 5 a), defined as the ratio between the electrical produced power and the total input power, equal to 29.4% with a value of direct normal irradiance equal to 1.0 kW/m^2. The relative efficiency calculated as the ratio between the electrical produced power and the only impinging power on the receiver (collected power), rises up to 31.2% always with reference to 1 kW/m^2 of direct normal irradiance. This value has to be compared with the 33% nominal performance obtainable for the receiver made with the cells considered (and shows that almost all the cells in the receiver are working approximately at their theoretical maximum. As can be easily understood, the electrical efficiency of the system depends on the value of direct normal irradiance: for instance, in case of a value of DNI equal to 0.1 kW/m^2, the electrical efficiency reduces to 27.4%. This evidence clearly highlights that the electrical efficiency trend is quite constant with the change in irradiance. Further, the thermal efficiency of the system (Figure 5) shows a variation from 66.8% (in case of DNI equal to 0.1 kW/m^2) to 64.8% (with reference to DNI equal to 1.0 kW/m^2). The reduction of the thermal efficiency with the increase of the direct normal irradiance can be explained considering the increase of electrical efficiency. This evidence allows to affirm that also this parameter does not show heavy changes with the irradiance variation.

The total amount of fossil fuel saving (FFS) due to use of SOLARIS concentrator as function of the direct normal irradiance can be estimated by considering the following relationship:

$$FFS = \frac{E_{EL}}{\eta_{EL,R}} + \frac{E_{TH}}{\eta_{TH,R}} \quad (1)$$

where E_{EL} and E_{TH} are respectively the net electrical and thermal produced energy (with reference to one hour of operation) of the system, while $\eta_{EL,R}$ and $\eta_{TH,R}$ are the electrical and thermal efficiency chosen as reference to compare the SOLARIS concentrator, in CHP application, with the separate generation of electricity and heat. In this study, a reference value for the electrical and thermal efficiency respectively 47.6% and 80.0% have been selected [24].
Further the avoided emissions of CO2 can be estimated, by assuming that 2.75 kg of CO_2 are produced per 1 kg of burned CH4. The results of FFS and CO_2 avoided emissions are respectively presented in Figure 6 and in Figure 7. From these figures it can be observed that, by assuming the nominal performance DNI equal to 1.0 kW/m^2, the achieved saving in fossil fuel and the corresponding CO_2 prevented emissions are respectively equal to about 50 kWh and 10 kg.
Finally, the nominal performance of the SOLARIS concentrator have been compared to the design electrical and thermal efficiency of a large number of existing and consolidated technologies usually adopted in CHP application with a produced electrical power equal or lower than 100 kW, such as internal combustion engines (ICE), micro gas turbines (MGT), Stirling engines (SE) and micro Rankine cycle (MRC) [25]. The result of the comparison if presented in Figure 8: it can be observed that the electrical and thermal efficiency of the SOLARIS concentrator can be compared with the internal combustion engines actually on the market.

4. CALCULATION MODEL AND ASSUMPTIONS

In order to estimate the performance of the system in Figure 2, under both the energetic and economic point of view, a parametric analysis has been developed by varying the number of residential utilities served by the solar concentrator. More in details, the SOLARIS concentrator has been included into a grid, connected to the national electric distribution network, with the aim of producing electrical, thermal and cooling energy for a group of residential utilities. In Figure 9 a schematic of the simulated grid is shown, including the SOLARIS concentrator in CHP application, an auxiliary boiler and a compressor chiller. Further, as it can be seen from the figure, an (i) electrical storage system and a (ii) thermal storage tank have been included in the calculation in order to minimize the exchange of electrical energy with the grid and the consumption of the fuel for the boiler. In particular for what regards the storage efficiency of electrical energy an average value of 60% was taken into account.
An in-house-developed calculation code has been developed in Excel VBA environment with the aim of estimating the energetic and the economic performance of the grid in Figure 9. The developed code is a mixed numerical-empirical tool, based on a lumped model approach. Each system component is considered as a black box, with a reduced number of key parameters, simulated with characteristic performance curves. These curves are obtained, when available, from experiments, or from physical modeling equations. The main input of the model are: (i) the user demand time profiles, (ii) the operating boundary conditions (ambient conditions, geographical position, etc.), (iii) the regulation strategy and the (iv) components parameters. The main output of the model are the energy fluxes, the efficiencies of each components and the economic performance of the SOLARIS concentrator.
For each domestic utilities, the following assumptions have been taken into account: (i) yearly required electrical, thermal and cold energy equal respectively to 3200 kWh, 20000 kWh and 3500 kWh (corresponding to about 1000 kWh of electrical energy) [26]. More in details, the electrical, thermal and cooling load of each household has been estimated for an entire year with reference to 8760 hours. The adopted electrical load curve is the result of the overlap of the various appliances which, in average, can be found in an Italian house; lighting, computer sites, cold and hot appliances, cleaning appliances, and audiovisual sites, were considered; also the stand-by mode was taken into account for the estimation of the electrical load curve. The thermal load curve, instead, is the sum of space heating and hot water demand; it was assumed that hot water demand is almost constant during the entire year being not influenced by the ambient air temperature or by the season, while the space heating demands is strictly dependent on the external temperature. More details on the household load profile can be found in [27].
The solar radiation has been estimated according to a latitude equal to 44.51 deg and longitude to 11.35 deg (corresponding to Bologna location) [28]. This calculation has been carried out by means of a routine, which is able to estimate (considering an entire year of operation – 8760 hours) the position of the sun, the direct and diffused radiation components incident on a horizontal surface, the direct, diffused and reflected radiation components incident on the SOLARIS concentrator. More details about the adopted physical-mathematical model can be found in an Authors' previous work [29].
Finally, the performance of the solar concentrator have been calculated on the basis of the curves in Figure 3, in Figure 4, and in Figure 5, while the batteries behavior is performed considering non-dimensional curves related to main parameters (i.e. maximum power in charging mode or in discharging mode, battery voltage, etc.) as function of the state of charge (SOC). Once the battery storable energy is defined, the main parameters can be estimated by means of curves obtained by interpolating the main characteristics of a wide range of batteries available on the market [30].

5. ENERGETIC PERFORMANCE EVALUATION

With reference to the scheme in Figure 9, the SOLARIS concentrator produced and the self-consumed electrical energy amounts are presented in Figure 10, as function of the number of considered utilities. In this figure, also the electrical energy purchased from the network is drawn. Further, the ratio of the self-consumed electrical energy to (i) the total amount of energy produced by the SOLARIS concentrator and to (ii) the electrical energy required by the considered utilities is drawn in Figure 11. In the same figure, the ratio between the electrical energy purchased from the network and the total amount of energy required by the utilities is also presented.

From Figure 4, it can be seen that being constant the SOLARIS concentrator produced electrical energy, the amount of self-consumed energy increases with the number of served utilities. The self-consumed energy is the sum of the fraction of SOLARIS concentrator produced energy which is directly sent to the utilities and of the energy initially stored into the batteries and then used to cover the energy demand. Also the total amount of energy purchased from the national distribution network, as expected, increases with the number of utilities: it should be noted that in case of one or two utilities this value is equal to zero, while increases up to about 2000 kWh/year and to slightly less than 10000 kWh/year respectively in case of three and five utilities (see Figure 10). With reference to Figure 11, the previous considerations allows to highlight that the SOLARIS concentrator can completely satisfy the electrical needs in case of one or two utilities and covers about the 84% of the electricity demand if three utilities are connected. The remaining fraction of the electricity demand (16%) is then covered by purchasing energy from the national distribution network. The ratio between self-consumed energy and demand decreases to the 53% in case of five considered utilities.

On the other side, considering the ratio between the self-consumed electrical energy and the total amount of electrical energy produced by the SOLARIS concentrator, it can be noted that this value is equal to 29% and to 53% in case of one and two utilities. The 73% of produced electrical energy is instead self-consumed if three utilities are taken into account. This percentage, for a number of utilities greater than three, slightly increases reaching a value of 75% and 77% respectively in case of four and five utilities. Always referring to the scheme in Figure 9, it can be observed that the remaining amount of the produced energy is stored into batteries without being used for the utilities or it is lost due to their storage efficiency. On this regard, the graph in Figure 12 shows the total amount of electricity sent to the batteries by dividing it between (i) the fraction used for the utilities demand, (ii) the losses and (iii) the stored energy which is not used. It can be observed from the figure that this last fraction becomes equal to zero if three utilities or more are taken into account. Further, as expected, the total energy sent to the batteries decreases with the increase of the utilities units.

For what concerns the utilities heat demand for space heating and hot water production, in Figure 13 the SOLARIS concentrator produced and the self-consumed thermal energy is presented as function of the number of considered utilities. Also the auxiliary boiler production is presented in this figure. Further, as already presented for the electrical energy, the ratio of the self -consumed thermal energy to (i) the total production of SOLARIS concentrator and to (ii) the utilities demand is drawn in Figure 14. In this case it can be observed that, unless the case with only one utility, the SOLARIS concentrator thermal production is not able to cover the heat demand of every utilities. Also in this case (see Figure 9), the self-consumed energy is equal to the sum of the term directly sent from the SOLARIS concentrator to the utilities and of the energy initially stored and then used in a later time. It can be noted, that in this case the losses of the thermal storage are negligible respect to the electrical storage losses: this explains why the produced energy and the self-consumed terms (Figure 13) appear almost coincident for a number of utilities equal or greater than two. In other words (Figure 14) the 100% of the SOLARIS concentrator thermal production can be recovered to partially cover the heat demand of two or more utilities. For instance, with three utilities, the SOLARIS concentrator allows to satisfy the 56% of the total demand, while the auxiliary boiler covers the remaining 44%. The boiler contribution rises up to the 66% of the heat demand in case of five utilities.

The above considerations make it possible to identify as three the number of utilities that will optimize the energy flows in order to maximize the self-consumed thermal and electrical energy, on one side, and to minimize both the purchasing from the national distribution network and the use of the boiler, on the other side. In fact, it can be considered that with two utilities a fraction of the electrical energy stored into the batteries is not used to satisfy the demand (see Figure 12), while with four utilities the boiler should cover slightly less than the 60% of the heat demand (see Figure 14).

6. ECONOMIC ANALYSIS

The economic analysis was conducted in order to identify the maximum capital cost that can be paid off in ten or in twenty years. More in details, for each of the analyzed cases was estimated the annual savings achievable by the non-purchase of electricity and gas to the boiler.

By considering the following relationship:

$$NPV = -C + \sum_{n=1}^{n_{max}} \frac{F_n}{(1+i)^n} \quad (2)$$

being:

NPV: net present value;
C: capital cost;
F_n: annual cash flow;
n_{max}: maximum year of operation (equal to 10 o to 20)
i: discount rate.

The maximum capital cost can be calculated by equating to zero the above expression; it follows:

$$C_{max} = \sum_{n=1}^{n_{max}} \frac{F_n}{(1+i)^n} \quad (3)$$

where the cash flow can be expressed as:

$$F_n = \left(E_{EL,u} - E_{EL}\right) \cdot \zeta_{EL} + \left(M_{g,u} - M_g\right) \cdot \zeta_g \quad (4)$$

being:

$E_{EL,u}$: the total electrical energy required by the utilities [kWh];
E_{EL}: the total electrical energy produced by the SOLARIS concentrator system and self-consumed by the utilities [kWh];
$M_{g,u}$: the total amount of natural gas used in the boiler to produce the yearly thermal energy demand of the utilities [Sm^3];
M_g: the amount of natural gas burned into the boiler when the SOLARIS concentrator is used [Sm^3];
ζ_{EL}: the cost of electrical energy [€/kWh];
ζ_g: the cost of natural gas [€/Sm^3].

For this analysis, the cost of electrical energy and natural gas were chosen respectively 250 €/MWh and 0.45 €/Sm3. Further, the discount rate was assumed to be 8%. The results of the economic analysis are presented in Figure 15.
The results show that a capital cost equal to about 31˙000 € (10 years) or slightly lower than 46˙000 € (20 years) can be achieved. From the figure it can be observed that the increase in the maximum capital cost becomes negligible with a number of utilities greater than three. In fact, with reference to 3 utilities, the maximum sustainable capital cost of the system is equal to about 30˙000 € in case of 10 years of return of the investment or 44˙000 if 20 years are taken into account. This last evidence confirms that three utilities are the optimum choice under both the energetic and the economic point of view.
Further, it should be taken into account that in many country, such as Italy, the production of electrical energy from renewable source is strongly incentivized. This additional economic advantage can obviously increase, depending on its amount, the values presented in Figure 15.
This last analysis clearly indicates that the development of renewable generators and consequently of storage systems could have a market in household sector only if the costs of these technologies will show a sensible decrease in the next upcoming years.

7. CONCLUDING REMARKS

In this study, a new concept of photovoltaic solar concentrator based on non-conventional mirrors coupled with high efficiency triple-junctions cells has been analyzed and discussed. An analytical study considering residential utilities has been performed in order to assess the energetic and economic performance of the system. Results suggest that the proposed system can optimize the electrical and thermal fluxes in case of 3 residential utilities minimizing the exchange of electrical energy with the grid and allowing the total recovery of the produced thermal energy. The economic analysis which has been developed indicates that the maximum sustainable capital cost of the system ranges between 30˙000 € and 44˙000 € depending on the years which are considered for the return of the investment.

REFERENCE

[1] Khamooshi M, Salati H, Egelioglu F, Faghiri AH, Tarabishi J, Babadi S. A Review of Solar Photovoltaic Concentrators. Int. J. of Phot. (2014). doi:10.1155/2014/958521

[2] Wiesenfarth M, Helmers H, Philipps SP, Steiner M, Bett AW. Advanced concepts in concentrating photovoltaics (CPV). In: Proc. of 27th European photovoltaic solar energy conference and exhibition, Frankfurt (Germany); 2012. p. 11–5.

[3] Martin A. Green, Keith Emery, Yoshihiro Hishikawa, Wilhelm Warta Ewan D. Dunlop Solar cell efficiency tables (Version 45) Prog. Photovolt: Res. Appl. 2015; 23:1–9

[4] A. Martì and A. Luque, Next Generation Photovoltaics: High Efficiency through Full Spectrum Utilization (Institute of Physics, Bristol, 2003).

[5] Benítez P, Miñano J, Zamora P, Mohedano R, et al. High performance Fresnel based photovoltaic concentrator. Opt Express 2010;18:A25–40. http://dx.doi.org/10.1364/OE.18.000A25.

[6] Singh PL, Sarviya RM, Bhagoria JL. Thermal performance of linear Fresnel reflecting solar concentrator with trapezoidal cavity absorbers. Appl Energy 2010;87(2):541–50. http://dx.doi.org/10.1016/j.apenergy.2009.08.019.

[7] Ryu K, Rhee JG, Park KM, Kim J. Concept and design of modular Fresnel lenses for concentration solar PV system. Solar Energy 2006;80(2):1580–7. http://dx.doi.org/10.1016/j.solener.2005.12.006.

[8] Verlinden P, Lewandowski A, Bingham C, Kinsey G, Sherif R, Lasich J. Performance and Reliability of Multijunction III-V Modules for Concentrator Dish and Central Receiver Applications. Photovoltaic Energy Conversion, Proc. of the 2006 IEEE 4th World Conference on Photovoltaic Energy Conversion: 592-597. doi:10.1109/WCPEC.2006.279526

[9] Chayet H, Kost O, Moran R, Lozovsky I. Efficient, low cost dish concentrator for a CPV based cogeneration system. In: AIP conference proceedings, vol. 1407; 2011. p. 249–52. http://dx.doi.org/10.1063/1.3658337.

[10] Lasich JB, Verlinden PJ, Lewandowski A, Edwards D, et al. World's first demonstration of a 140 kWp heliostat concentrator PV (HCPV) system. In: 34th IEEE photovoltaic specialists conference (PVSC), 2009. p. 002275–80. http://dx.doi.org/10.1109/PVSC.2009.5411354

[11] G. Zanganeh, R. Bader, A. Pedretti, M. Pedretti, A. Steinfeld, A solar dish concentrator based on ellipsoidal polyester membrane facets, Solar Energy 2012;86(1):40-47. http://dx.doi.org/10.1016/j.solener.2011.09.001.ù

[12] Baig H, Heasman KC, Mallick TK. Non-uniform illumination in concentrating solar cells. Renew Sustain Energy Rev 2012;16(8):5890–909. http://dx.doi.org/10.1016/j.rser.2012.06.020.

[13] Salemi A, Eccher M, Miotello A, Brusa RS. Dense array connections for photovoltaic systems. Prog Photovolt: Res Appl 2011;19(4):379–90. http://dx.doi.org/10.1002/pip.1040.

[14] Loeckenhoff R, Kubera T, Rasch KD. Water cooled TJ dense array modules for parabolic dishes. In: AIP conference proceedings, vol. 1277; 2010. p. 43–6. http://dx.doi.org/10.1063/1.3509229.

[15] Burkhard DG, Shealy DL. Design of reflectors which will distribute sunlight in a specified manner, Sol. En. 1975; 17(4): 221-227

[16] Chong KK, Wong CW, Siaw FL, Yew TK. Optical Characterization of Nonimaging Planar Concentrator for the Application in Concentrator Photovoltaic System. J. Sol. Energy Eng 2010; 132(1) n. 011011. doi:10.1115/1.4000355

[17] Fu L, Leutz R, Annenn HP. Evaluation and comparison of different designs and materials for Fresnel lens-based solar concentrators. Proc. SPIE 8124, Nonimaging Optics: Efficient Design for Illumination and Solar Concentration VIII 2011; n.81240E. doi:10.1117/12.893390

[18] Hernández M, Cvetkovic A, Benítez P, Miñano JC. High performance Kohler concentrators with uniform irradiance on solar cell. Proc. SPIE 7059, Nonimaging Optics and Efficient Illumination Systems V 2008; n.705908. doi:10.1117/12.794927

[19] A. Giannuzzi, E. Diolaiti, M.Lombini, A. De Rosa, B. Marano, G. Bregoli, G. Cosentino, I. Foppiani, L. Schreiber Enhancing the efficiency of solar concentrators by controlled optical aberrations: method and photovoltaic application, Applied Energy 2015;145:211-222. http://dx.doi.org/10.1016/j.apenergy.2015.01.085

[20] Noll R. Zernike polynomials and atmospheric turbulence. J. Opt. Soc. Am. 1976; 66(3): 207-211.

[21] www.azurspace.com

[22] Royne A, Christopher JD. Design of a jet impingement cooling device for densely packed PV cells under high concentration. Sol. En. (2007); 81(8): 1014-1024. *doi: 10.1016/j.solener.2006.11.015*

[23] Zhu L, Boehm RF, Wang Y, Halford CK, Sun Y. Water Immersion Cooling of PV Cells in a High Concentration System. *Sol.* Energ. *Mat. Sol.* Cells; 95(2): 538-545. doi:10.1016/j.solmat.2010.08.037

[24] European Enviromental Agency "Efficiency of conventional thermal electricity and heat production (ENER 019)" Jan 2015"

[25] Bianchi M., De Pascale A., Melino F., Peretto A., "Performance prediction of micro-CHP System using simple virtual operating cycles" Applied Thermal Engineering, Volume 71, 2014, Pages 771-779

[26] Barbieri E. S., Melino F., Morini M., "Influence of the Thermal energy storage on the Profitability of Micro-CHP Systems for Residential Building Applications", Applied Energy, Volume 97, September 2012, Pages 714–722

[27] Bianchi M., Ferrari C., Melino F., Peretto A., "Feasibility study of a Thermo – Photo – Voltaic system for CHP application in residential buildings", Applied Energy, Volume 97, September 2012, Pages 704–713

[28] Antonucci V., Brunaccini G., De Pascale A., Ferraro M., Melino F., Orlandini V., Sergi F., "Integration of □-SOFC generator and ZEBRA batteries for domestic application and comparison with other □-CHP technologies", Proceedings of 7th International Conference on Applied Energy – ICAE 2015 – March 28 - 31, 2015, Abu Dhabi, United Arab Emirates

[29] Bianchi M., Branchini L., De Pascale A., Melino F. "Storage Solutions for Renewable Production in Household Sector", Energy Procedia, Volume 61, 2014, Pages 242-245

[30] Bianchi M., Branchini L., Ferrari C., Melino F., "Optimal size of grid-independent hybrid photovoltaic-battery power systems for household sector", Applied Energy, Applied Energy 136 (2014) 805 – 816

FIGURE CAPTIONS

Figure 1. Effects introduced in the solar image by the indicated polynomials
Figure 2. Mechanical shaded model of the SOLARIS concentrators and zoom of the focal zone showing the irradiance pattern and the receiver scheme
Figure 3. Power collected by the concentrator (input power) and the light effectively impinging on the array (collected power) of the SOLARIS concentrator as function of DNI at the collector aperture
Figure 4. Produced electrical and thermal power of the SOLARIS concentrator as function of DNI at the collector aperture
Figure 5. Net thermal (a) and electrical (b) efficiency of the SOLARIS concentrator as function of DNI at the collector aperture
Figure 6. Fossil fuel saving of the SOLARIS concentrator as function of DNI at the collector aperture
Figure 7. CO_2 avoided emissions of the SOLARIS concentrator as function of DNI at the collector aperture
Figure 8. Thermal efficiency vs electric efficiency for micro CHP technologies compared to SOLARIS concentrator
Figure 9. Schematic of the simulated grid including the SOLARIS concentrator
Figure 10. SOLARIS concentrator produced electrical energy, self-consumed for the utilities and purchased from the network
Figure 11. Electrical energy balance
Figure 12. Energy balance of batteries
Figure 13. SOLARIS concentrator produced thermal energy, self-consumed for the utilities and produced from the boiler
Figure 14. Thermal energy balance
Figure 15. SOLARIS concentrator maximum sustainable capital cost as function of the number of served utilities

TABLE CAPTIONS

Table 1. 2D and 3D representations of the main polynomials involved in the modelling

FIGURES

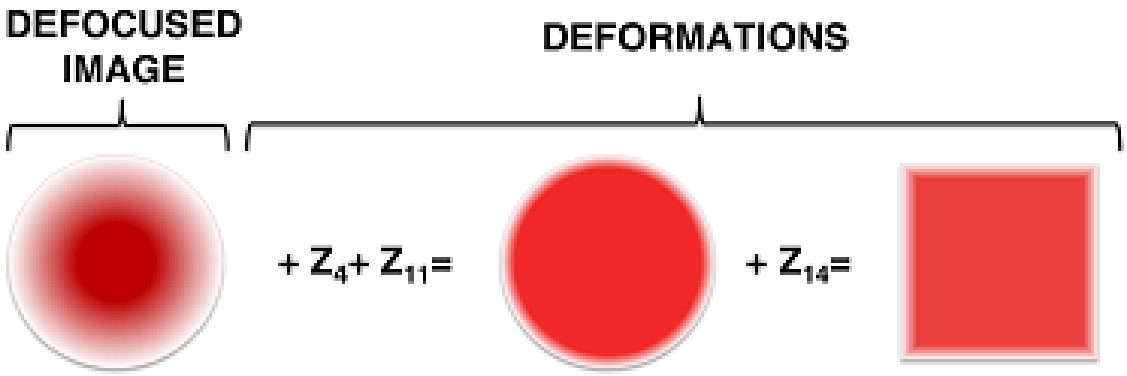

Figure 1. Effects introduced in the solar image by the indicated polynomials

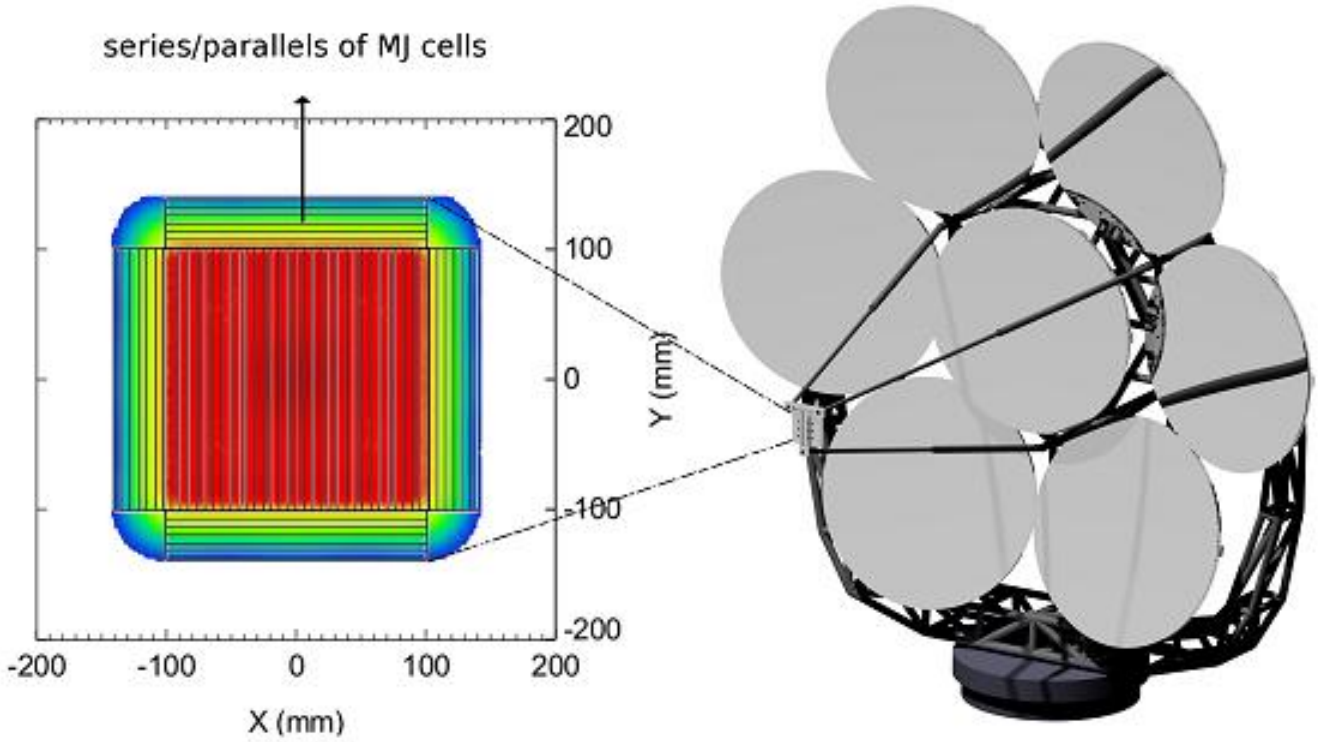

Figure 2. Mechanical shaded model of the SOLARIS concentrators and zoom of the focal zone showing the irradiance pattern and the receiver scheme

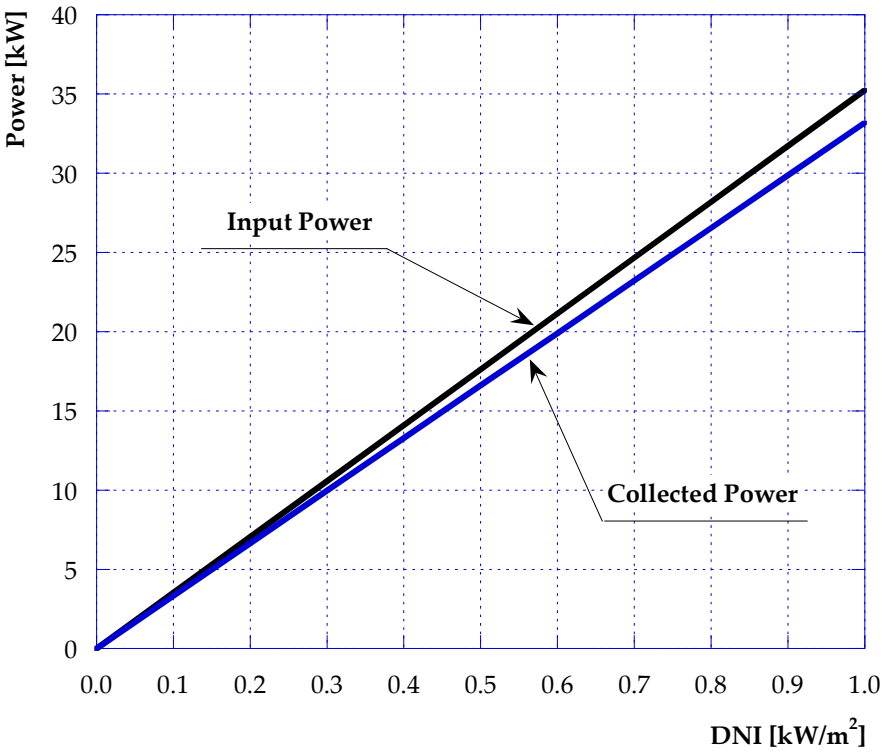

Figure 3. Power collected by the concentrator (input power) and the light effectively impinging on the array (collected power) of the SOLARIS concentrator as function of DNI at the collector aperture

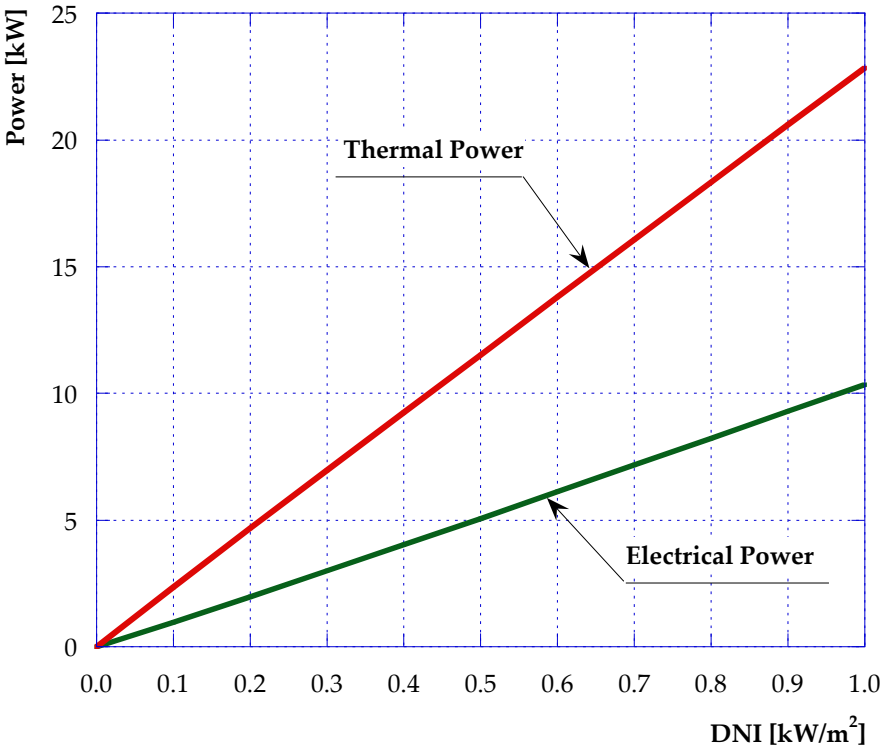

Figure 4. Produced electrical and thermal power of the SOLARIS concentrator as function of DNI at the collector aperture

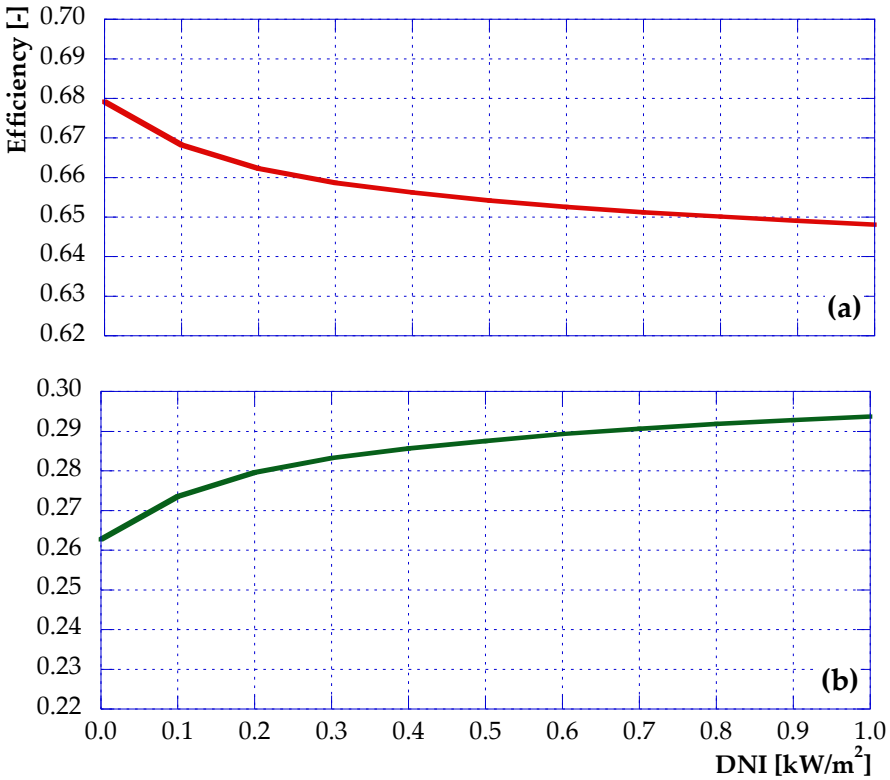

Figure 5. Net thermal (a) and electrical (b) efficiency of the SOLARIS concentrator as function of DNI at the collector aperture

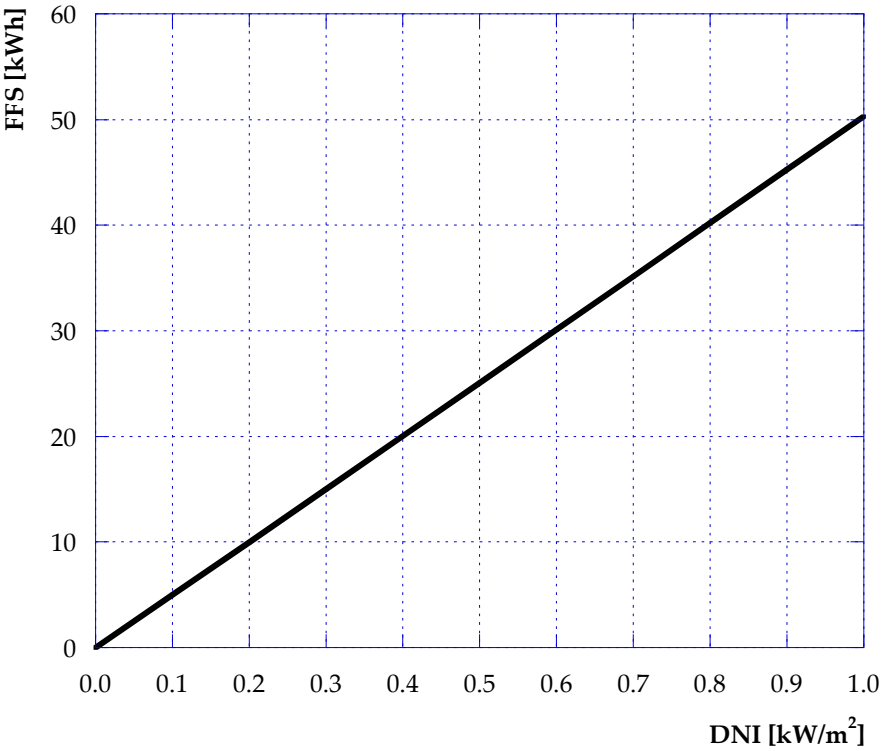

Figure 6. Fossil fuel saving of the SOLARIS concentrator as function of DNI at the collector aperture

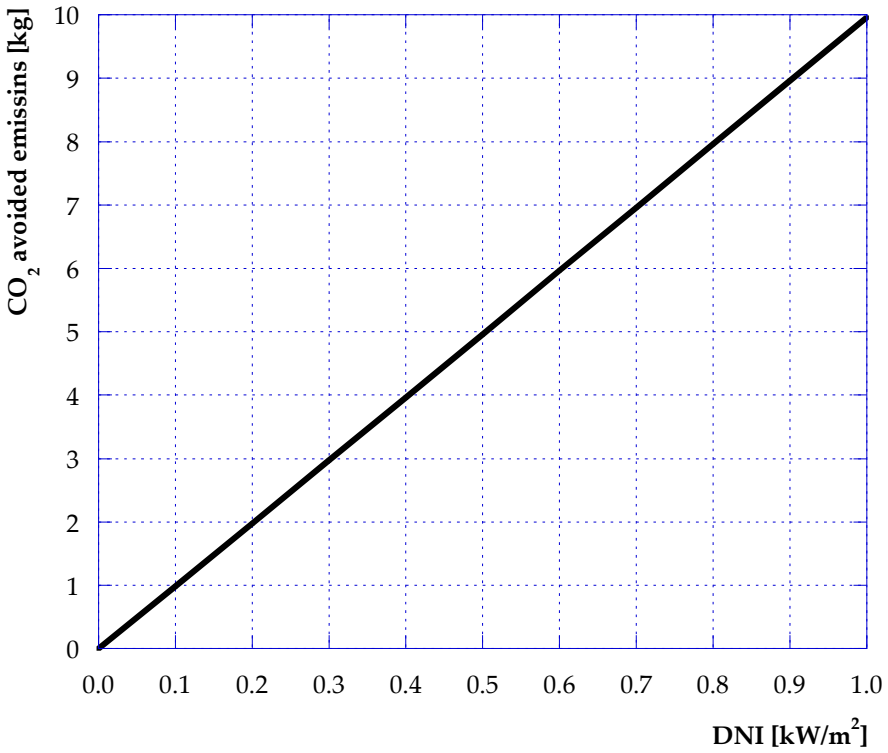

Figure 7. CO_2 avoided emissions of the SOLARIS concentrator as function of DNI at the collector aperture

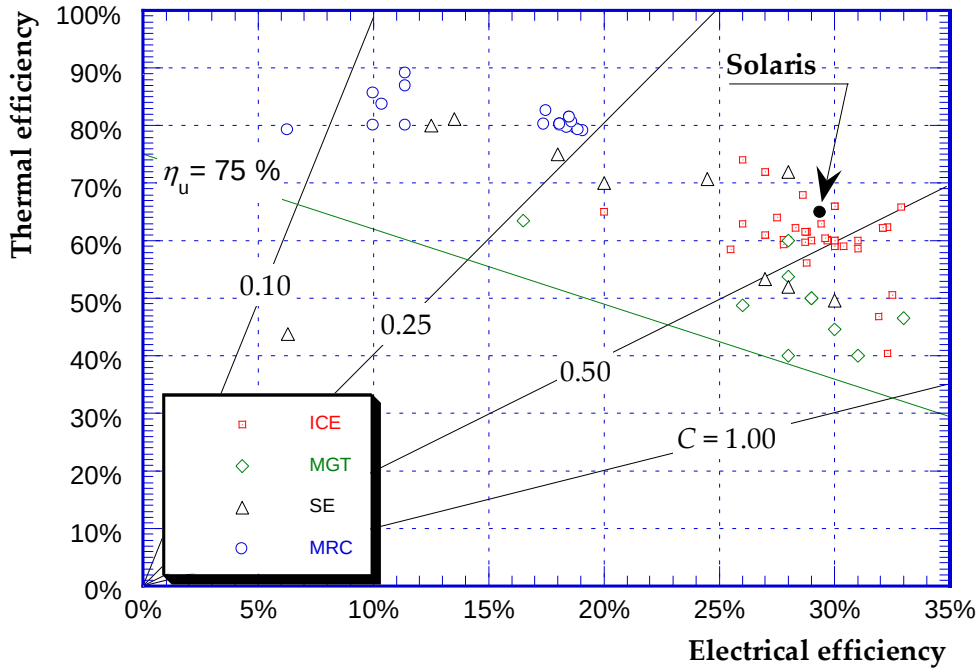

Figure 8. Thermal efficiency vs electric efficiency for micro CHP technologies compared to SOLARIS concentrator

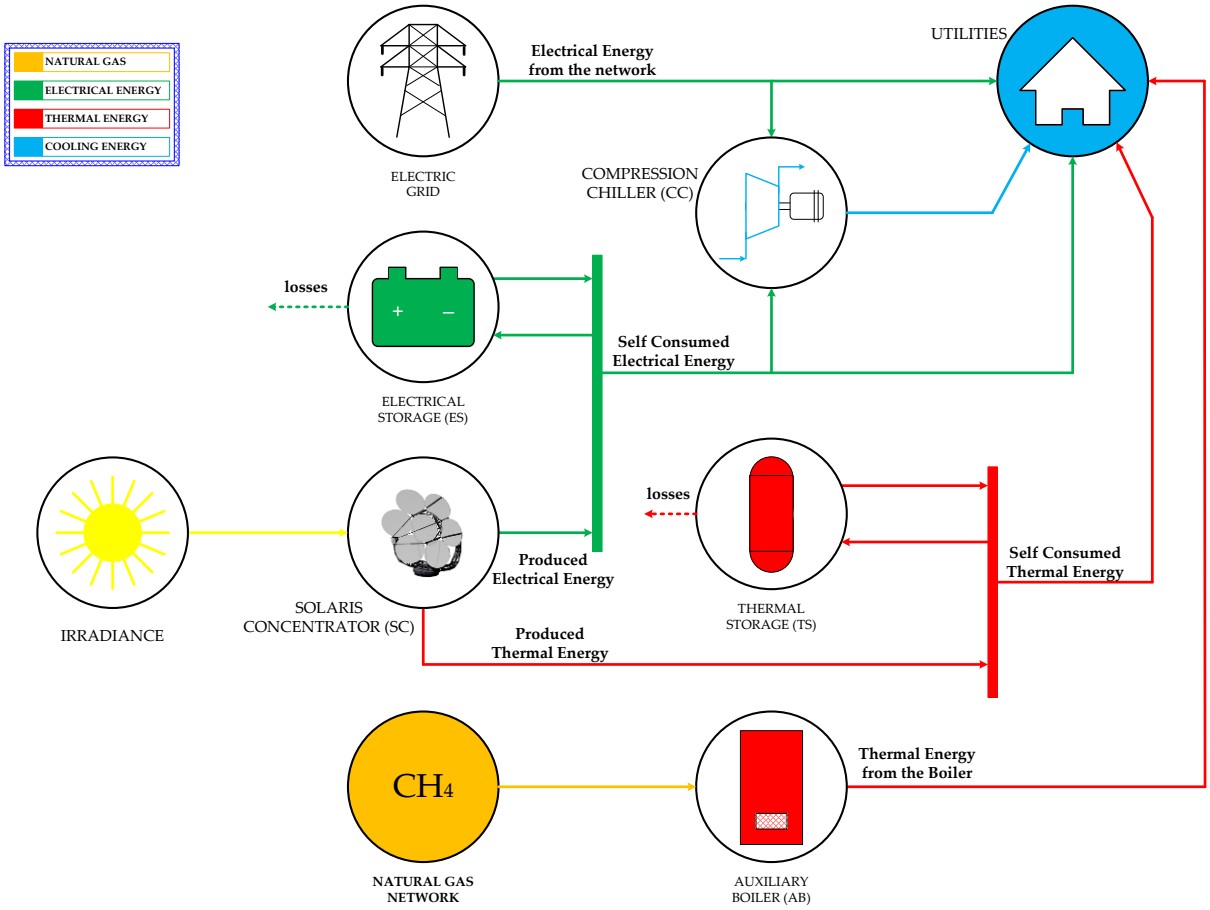

Figure 9. Schematic of the simulated grid including the SOLARIS concentrator

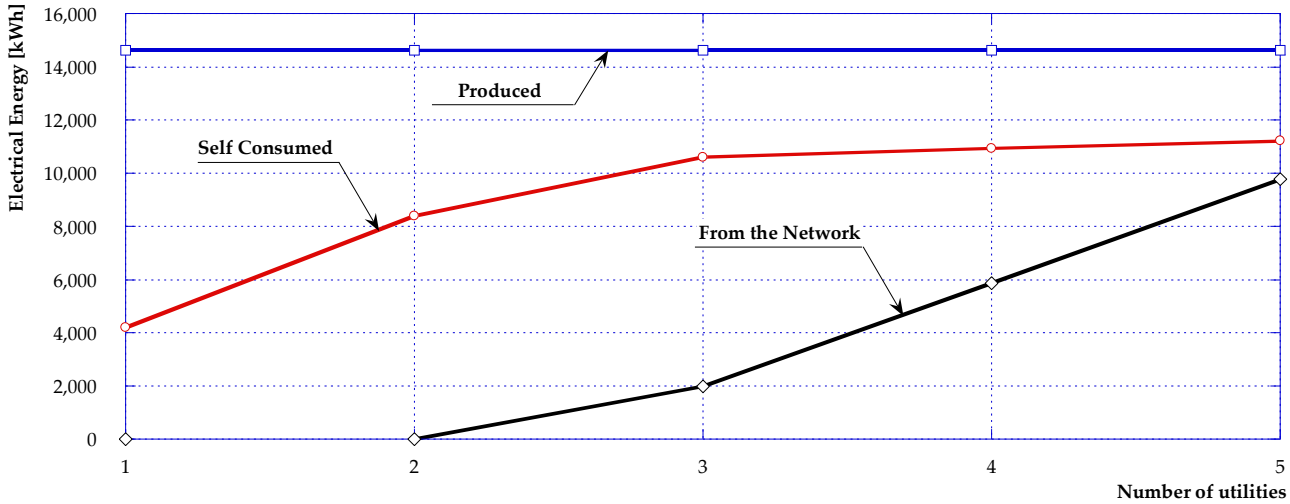

Figure 10. SOLARIS concentrator produced electrical energy, self-consumed for the utilities and purchased from the network

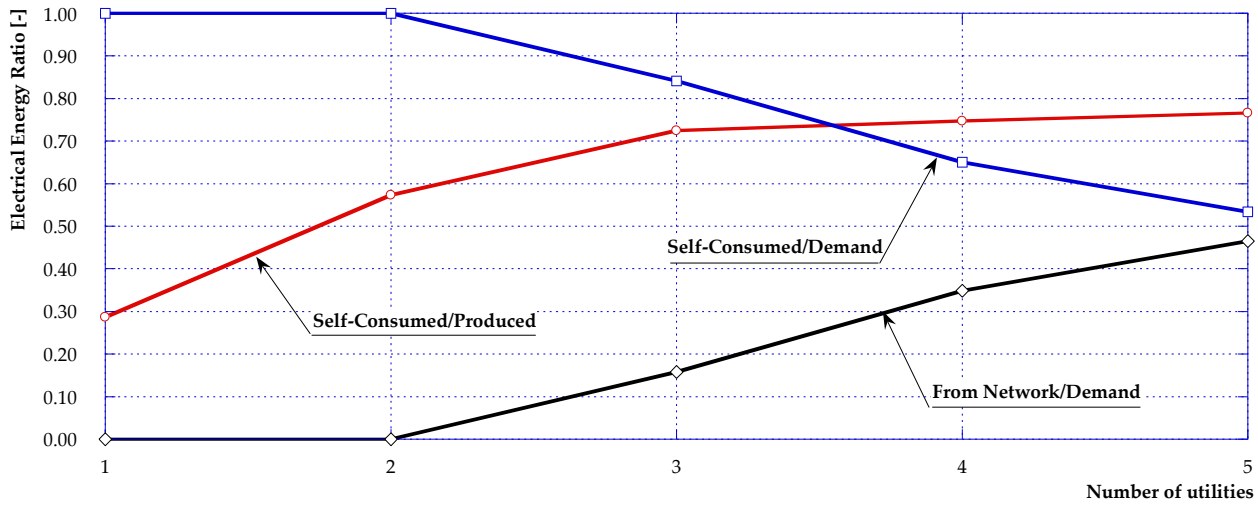

Figure 11. Electrical energy balance

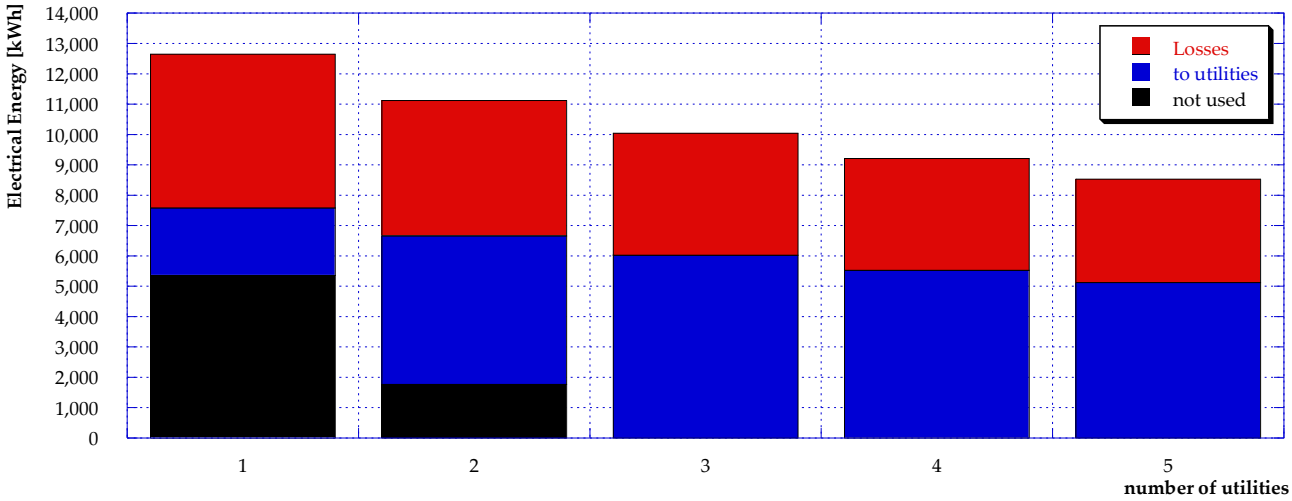

Figure 12. Energy balance of batteries

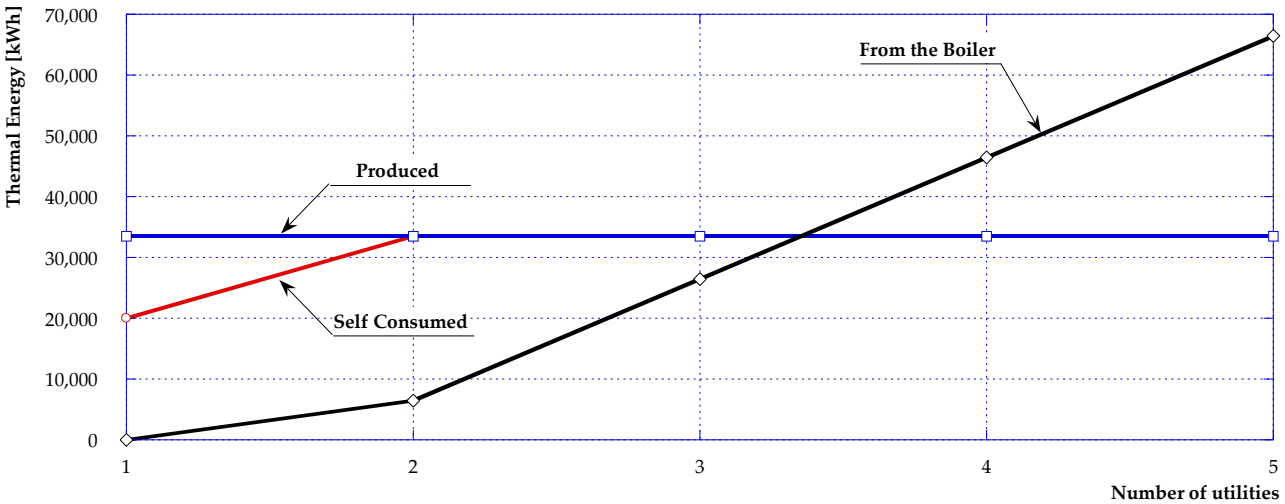

Figure 13. SOLARIS concentrator produced thermal energy, self-consumed for the utilities and produced from the boiler

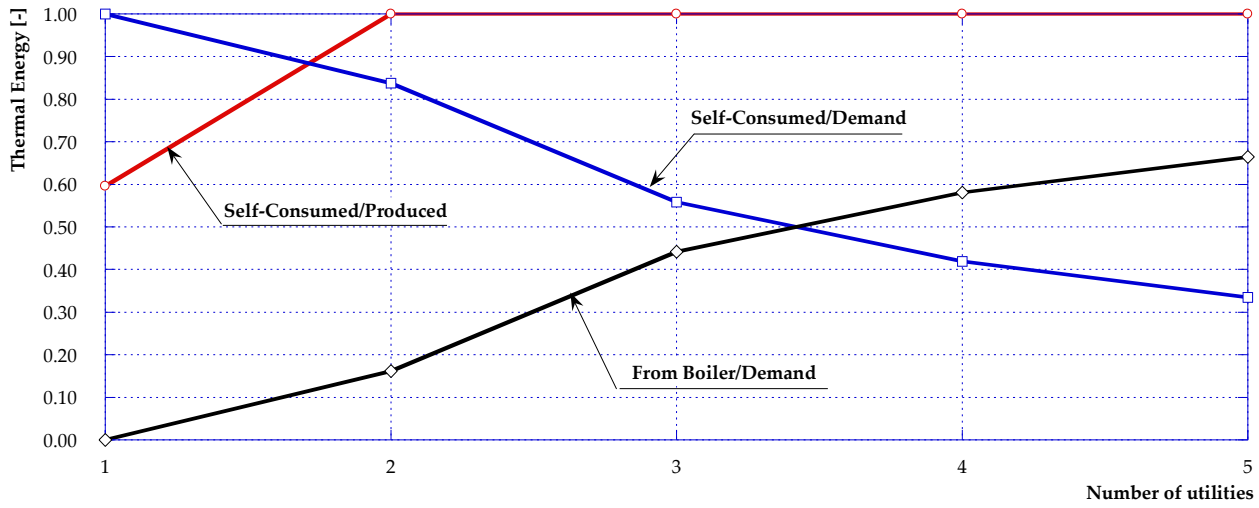

Figure 14. Thermal energy balance

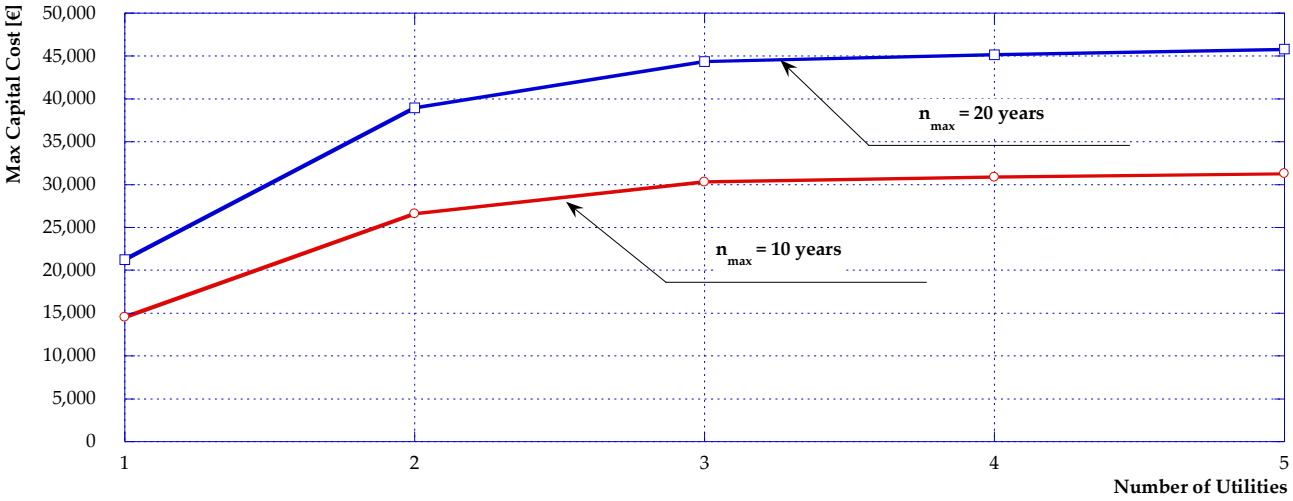

Figure 15. SOLARIS concentrator maximum sustainable capital cost as function of the number of served utilities

TABLES

Table 1. 2D and 3D representations of the main polynomials involved in the modelling

	Zernike mode		
	4^{th}	11^{th}	14^{th}
2D	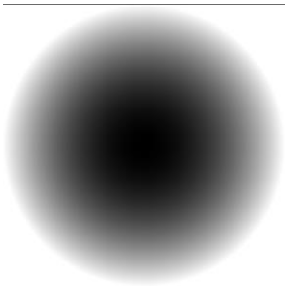	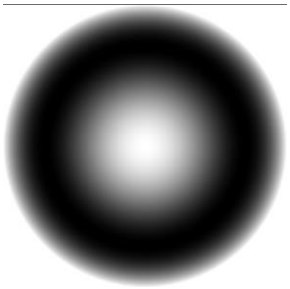	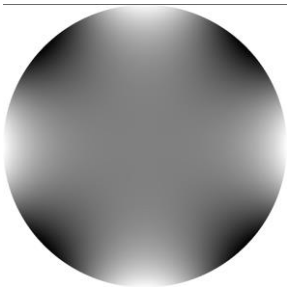
3D